DOI: 10.26599/FSHW.2024.9250132

Contents lists available at SciOpen

Food Science and Human Wellness

journal homepage: https://www.sciopen.com/journal/2097-0765

Rice Bran-derived Peptide KF-8 Attenuates Dexamethasone-induced Myopathy in *Caenorhabditis elegans* by Regulating Locomotion-related Genes

Yixin Wu[1], Jianqiang Wang[1], Fang Huang[1], Yajuan Chen[1], Qinlu Lin[1], Zhongxu Chen[1], Zhigang Liu[4], Yao Jiang[5], Wenqing Xie[2], Hengzhen Li[2], Yusheng Li[2,3*], Ying Liang[1*]

[1]*Molecular Nutrition Branch, National Engineering Research Center of Rice and By-product Deep Processing, College of Food Science and Engineering, Central South University of Forestry and Technology, Changsha 410004, Hunan, P.R. China.*

[2]*Department of Orthopedics, Xiangya Hospital, Central South University, Changsha, Hunan, P.R. China.*

[3]*National Clinical Research Center for Geriatric Disorders, Xiangya Hospital, Central South University, Changsha, Hunan, P.R. China.*

[4]*Laboratory of Functional Chemistry and Nutrition of Food, College of Food Science and Engineering, Northwest A&F University, Yangling, Shaanxi, 712100, P.R. China*

[5]*The Key Lab of Non-wood Forest Cultivation and Protection of Education Ministry, The Key Lab of Non-wood Forest Products of Forestry Ministry, Forestry Institute, Central South University of Forestry & Technology, Changsha 410004, Hunan, China.*

ABSTRACT: Background and aims: Dexamethasone is a common glucocorticoid medication with adverse effects that can cause muscle atrophy, but no drug intervention has been approved or recommended for this condition. KF-8 is a rice bran-derived anti-oxidant peptide that extends the life span of *Caenorhabditis elegans*. **Methods**: We established a *C. elegans* model of dexamethasone-induced myopathy to evaluate the potential therapeutic effects of KF-8 in this model. *C. elegans* muscle function was assessed in terms of locomotory behaviors including crawling, swimming, burrowing, pharyngeal pumping, and head swing. Muscle actin filament integrity was evaluated using fluorescence imaging. The molecular mechanisms of KF-8 were investigated using transcriptome sequencing, qRT-PCR, RNA interference, and western blot analysis. **Results:** Dexamethasone disrupted actin filaments in the striated muscles of the body wall and inhibited *C. elegans* crawling, swimming, burrowing, pharyngeal pumping, and head swing. KF-8 reversed the actin filament disruption and locomotor dysfunction induced by dexamethasone. Transcriptome sequencing, pathway enrichment, and qRT-PCR analyses revealed that KF-8 regulated the locomotion-related genes *W04G5.10*, *vha-12*, and *ddr-1*, as well as *age-1* (the catalytic subunit ortholog of PI3K), and *akt1*. RNA interference, conducted using a genetically engineered *E. coli* HT115 strain as a food source, confirmed *age-1* as a key regulator of locomotor function of *C. elegans*. Further mechanistic studies with C2C12 myotubes showed that KF-8 regulated the IRS-PI3K-Akt pathway, the master regulator of protein synthesis and degradation. **Conclusion:** Together, these findings suggest that KF-8 protects against dexamethasone-induced myopathy in *C. elegans* by regulating locomotion-related genes and the IRS-PI3K-Akt pathway.

Keywords: dexamethasone; myopathy; KF-8; IRS-PI3K-AKT

1. Introduction

Muscle atrophy or dysfunction is a common problem in the elderly [1, 2]. It also occurs in a variety of pathological conditions such as chronic obstructive pulmonary disease [3], cancer cachexia [4], and chronic

***Corresponding author**
Ying Liang; liangying498@163.com
Yusheng Li; liyusheng@csu.edu.cn

Received 22 November 2023
Received in revised from 28 January 2024
Accepted 5 March 2024

heart disease [5]. It can be caused by certain hormonal drugs such as glucocorticoids (GCs) [6]. GCs are a class of steroid hormones that are commonly used to fight inflammation or as immunosuppressive agents. GCs are known to have catabolic effects on skeletal muscles mainly by suppressing protein synthesis and promoting protein degradation. Sustained, elevated GC levels can lead to muscle wasting [7, 8]. Dexamethasone is the most commonly prescribed GC. Evidence has shown that continued use of dexamethasone can cause severe skeletal muscle damage through inhibiting the PI3K/AKT pathway [9–11]. The mainstay treatment options include reduction of the GC or switching to alternate, steroid-sparing therapies. Aerobic and resistance exercises have been recognized as an effective supportive management for GC-induced myopathy [12, 13]. However, excessive or eccentric exercise can exacerbate the loss of muscle function, and exercise is not always a feasible option for the elderly and people with severe physical impairments. A significant number of experimental agents such as branched-chain amino acids, creatine, androgens (testosterone and DHEA), and glutamine have been evaluated in animal models, but these agents have not been tested in humans and are not currently approved or recommended for the treatment of GC-induced myopathy [14].

Nutritional strategies such as supplementation with whey protein or essential amino acids can support muscle tissue regeneration after sports or exercise-caused injury [15, 16]. In addition, recent studies have shown that certain bioactive peptides can enhance muscular performance and reduce exercise-related muscle damage [17, 18]. However, whether these peptides have therapeutic benefits on GC-induced muscle atrophy remains unknown. Because bioactive peptides can be absorbed in their intact form via the digestive system, they can be administered as a dietary supplement. Rice bran protein, a protein derived from rice bran, is a functional ingredient in the development of nutritional foods [19]. KF-8 (Lys-His-Asn-Arg-Gly-Asp-Glu-Phe) is an 8-amino acid bioactive peptide derived from rice bran protein. Our previous studies have shown that the KF-8 peptide exhibits anti-oxidant properties and can reduce H_2O_2-induced damages in cultured human umbilical vein endothelial and NIH/3T3 cells [20, 21]. KF-8 also exhibits anti-inflammatory properties and can inhibit oxidative organ injuries in aging mice [21]. Accordingly, we speculated that KF-8 may have therapeutic benefits for treating dexamethasone-induced myopathy.

At present, rodent animal models have been primarily used to study dexamethasone-induced myopathy [22, 23]. However, *Caenorhabditis elegans* (*C. elegans*) could be a good candidate model organism to study drug-induced myopathy because of its short life cycle and similarities to humans at the molecular level. *C. elegans* also exhibits a more fixed behavior pattern compared with laboratory rodents, which is an advantage for muscle functional studies [24]. In this study, we successfully established a *C. elegans* model of dexamethasone-induced myopathy. We quantitatively evaluated the muscle structures and locomotor movements of *C. elegans* using imaging analyses and behavioral studies. Oxidative stress was assessed with common biomarkers, and the underlying molecular mechanisms were investigated using transcriptome sequencing, pathway enrichment, qRT-PCR, and western blot analyses, as well as RNA interference (RNAi).

2. Materials and Methods

2.1 Chemicals and reagents

Dexamethasone (99% pure) and dimethyl sulfoxide were purchased from Sigma (USA). KF-8 (purity > 99%) was purchased from China Peptides (China). Fetal bovine serum and DMEM high glucose medium were from BI (Israel). Trypsin-EDTA (0.25%), horse serum, and double antibiotic solution containing penicillin and streptomycin were from Thermo Fisher Scientific (USA). Levamisole hydrochloride, rhodamine phalloidin, total anti-oxidant capacity (T-AOC) and malondialdehyde (MDA) detection kits were from Solarbio Biotechnology Co., Ltd. (China). The BCA protein concentration kit and Phanta Max Super-Fidelity DNA Polymerase were purchased from Vazyme Biological Co., Ltd. (China). Superoxide dismutase (SOD) and glutathione peroxidase (GSH-Px) detection kits were purchased from Beyotime Biotechnology Co., Ltd. (China). The DCFH-DA fluorescent probe was from Meilun Biotechnology Co., Ltd. (China). The RIPA cracking buffer was purchased from Servicebio Biotechnology (China). All chemical reagents were of analytical grade unless stated otherwise. The DL 2000 Marker, QuickCut™ EcoR I, and QuickCut™ XhoI were from Takara (Japan). The Trans2K® Plus DNA Marker was from TransGen Biotech (China). The Agarose Gel Recovery kit and DNA Purification Recovery kit were purchased from Omega Bio-tek (USA). The Endotoxin Free Plasmid Medium Volume Extraction Kit was from Tiangen (China). The *E. coli* strains OP50 and HT115, and the pLVX-IRES-ZsGreen1 plasmid was purchased from Ori-Bio (China). Antibodies targeting MHC3 (22287-1-AP), IRS1 (17509-1-AP), PI3K (20584-1-AP), Akt (60203-2-Ig), p-mTOR (Ser2448) (67778-1-Ig), mTOR (66888-1-Ig), FOXO1 (18592-1-AP), P70(S6K) (14485-1-AP), FBXO32 (Atrogin-1) (67172-1-Ig), TRIM63 (Murf1) (55456-1-AP), and 4EBP1 (60246-1-Ig) and the goat anti-rabbit secondary antibody were purchased from Proteintech (USA). Antibodies targeting p-IRS1 (ab109543), p-PI3K (ab278545), and p-Akt (ab192623) were purchased from Abcam (UK). Antibodies targeting FLT3 (YT1730), ATP6V1B2 (YN1508), DDR1 (YT6127), p-P70(S6K) (YP1427), and p-4EBP1 (YP0001) were purchased from Immunoway (USA).

2.2 Dexamethasone and KF-8 treatment

Synchronized worms grown to the L4 stage were transferred to NGM plates containing 150 μmol/L pentafluorouracil (control) or 150 μmol/L pentafluorouracil and specific concentrations of dexamethasone. Pentafluorouracil was used to inhibit spawning. The worms were fed inactivated OP50 containing specific concentrations of the KF-8 peptide and cultivated for 36 h.

2.3 Rhodamine-phalloidin staining

After treatment, the worms were transferred into EP tubes. The worms were washed with M9 buffer by low-speed centrifugation, fixed in pre-cooled 1% paraformaldehyde for 10 min, again washed with M9 buffer, and permeabilized with pre-cooled acetone at – 20℃ for 2 min. After washing with M9 buffer, the worms were incubated with 100 nmol/L rhodamine phalloidin at room temperature for 2 h in the dark and then washed with M9 buffer. Droplets containing the *C. elegans* were loaded onto glass slides and photographed under a confocal laser microscope as previously described [25, 26].

2.4 Burrowing experiment

A single drop of 26%w/w pluronic F-127 solution was added to each well of a 48-well plate. After about 10 s, the worms were transferred into the wells. An additional 26%w/v pluronic F-127 solution was added dropwise to a liquid level of 0.8 cm, and the plate was allowed to stand undisturbed at room temperature for about 5 min to allow the solution to solidify. After 20 μL of OP50 was added as an attractant to the top surface of the gel, the plate was photographed every 15 min for a total of 90 min. The number of worms in each group that moved from the bottom to the top of the gel within 90 min was recorded as previously described [27, 28].

2.5 T-AOC, MDA, GSH-Px, and SOD detection

After treatment, the animals were transferred into EP tubes and washed twice with M9 buffer using low-speed centrifugation. After removal of the supernatant, the worms were mixed with either the extraction reagent or M9 buffer, according to instructions of the corresponding kits, and sonicated using an ultrasonic crusher set to 200w with a pulse length time of 5 s and a rest period of 10 s for a total of 7 min. After sonication, the homogenates were centrifuged at 4℃ and 7,000 g for 5 min. The supernatants were collected, and the T-AOC, MDA, GSH-Px, and SOD levels were determined using the corresponding detection kits following the manufacturers' instructions.

2.6 Total RNA extraction, integrity testing, and cDNA synthesis

After treatment, the worms were transferred into EP tubes and washed three times with M9 buffer. The worms were rapidly frozen using liquid nitrogen and thawed at room temperature. The freeze-thaw cycle was repeated five times, and the resulting lysates were centrifuged at 4℃ and 7,000 g for 10 min. The supernatants were transferred into EP tubes, mixed with chloroform, allowed to stand at room temperature for 5 min, and centrifuged at 4℃ and 8,500 g for 15 min. The supernatants were transferred to new tubes, mixed with isopropanol, allowed to stand at room temperature for 10 min, and again centrifuged at 4℃ and 8,500 g for 15 min. The supernatants were discarded, and the remaining RNA samples were washed with 80% ethanol using centrifugation at 4℃ and 7,000 g for 5 min. After the supernatants were removed, the samples were air-dried at room temperature and dissolved in RNA-free water. To extract RNA, the myotubes were washed 3 times with PBS buffer and mixed with Trizol extraction solution on ice. RNA was extracted using centrifugation as described above. The quality and purity of the RNA samples were determined using Nano-Drop, and the RNA integrity was evaluated using agarose gel electrophoresis.

2.7 Plasmid construction

The coding sequence of *age-1* was retrieved from the National Center for Biotechnology Information (NCBI). Primers for seamless cloning were designed using CE Design V. The coding sequence was amplified from *E. coli* cDNA using PCR with the following primers: forward, atggctagccacgtgacgcgtATGTGGAATAATCGAGATTTGTTCG; reverse, gtcgacggtatcgataagcttTCAGTAGTGTTTGACTGCGTGGA. The amplification reactions were carried out under the following conditions: 2 min at 95℃ for 1 cycle followed by 15 s at 95℃, 15 s at 60℃, and 1 kb/min at 72℃. The PCR products were resolved using agarose gel electrophoresis at 110 V for 30 min using the

DL2000 Marker as a control. The pLVX-IRES-ZsGreen1 plasmid vector and PCR products were both digested with MIuI and HindIII, and the linearized plasmid and digested PCR products were ligated for 15 min in a 50℃-water bath. The ligated plasmid was transduced into *E. coli* HT115 by incubation on ice for 30 min followed by heat-shock at 42℃ for 90 s and rapid ice bath cooling for 2 min. The transduced *E. coli* cells were incubated in antibiotics-free LB medium for 45 min at 37℃ on a 200-r/min shaker for recovery. The cells were then transferred to inverted flat dishes with LB agar containing ampicillin and incubated at 37℃ for 16 h to generate positive clones. The expression of *age-1* dsRNAs was confirmed using PCR.

2.8 Age-1 silencing

The HT115 strain transduced with either the blank control or *age-1* dsRNA-expressing plasmid was cultured in LB medium containing 50 μg/mL ampicillin and 0.2 mmol/L isopropyl-β-D-thiogalactoside (IPTG) overnight at 37℃. The bacterial suspension (300 μL) was transferred to NGM plates and allowed to air-dry overnight at 25℃. Synchronized worms were transferred to the above HT115-coated plates with or without 0.1 mmol/L KF-8 and cultivated to the adult stage. The worms were removed 4 h after they started laying eggs, and the eggs were hatched and grown until the adult stage. The second-generation adults were used for behavioral studies and mRNA expression analysis.

2.9 Western blot analysis

C2C12 myotubes were lysed in the presence of the protease inhibitor phenylmethylsulfonyl fluoride. After centrifugation, the supernatants were collected, and the protein concentrations were determined using the BCA method. Proteins were separated using gel electrophoresis and transferred to Immobilon®-P PVDF membranes (Sigma). After blocking for 1 h, the membranes were incubated with specific primary antibodies overnight at 4℃, washed, and incubated with the corresponding HRP-conjugated secondary antibody for 1 h at room temperature. The protein bands were visualized using an ECL reagent (Novizan), detected using an Azure c500 gel imager (Azure Bio systems, USA), and quantified using densitometric analysis with ImageJ. Data were normalized to β-actin.

2.10 Statistical analysis

All data were analyzed using SPSS21.0 software. The numerical information is given as means standard deviation (SD). Comparisons among several randomized groups were conducted using one-way ANOVA and Tukey post hoc test. Comparisons between groups were conducted using a student's *t-test*. The significance level was set at $P < 0.05$. GraphPad software was used to visualize the data.

3. Results

3.1 Dexamethasone causes myopathy in C. elegans

We first conducted behavior experiments measuring *C. elegans* crawling on NGM plates and swimming in water to investigate the effects of dexamethasone on muscle functions of *C. elegans*. As shown in Figure 1A–D, dexamethasone significantly decreased the crawling and swimming frequencies in a dose- and time-dependent manner. Rhodamine phalloidin is a high-affinity fluorescent probe for F-actin filaments in

muscles. In this study, rhodamine-phalloidin staining revealed breakages in striated muscles of the body wall after administration of 10 μmol/L dexamethasone, and the number of breakages increased with the dose and time of dexamethasone treatment (Fig. 1E − F). These findings were similar to previous findings on dexamethasone-induced loss in muscle mass and grip strength in mice [29, 30]. Thus, dexamethasone can induce myopathy in *C. elegans* similar to that in rodents and humans.

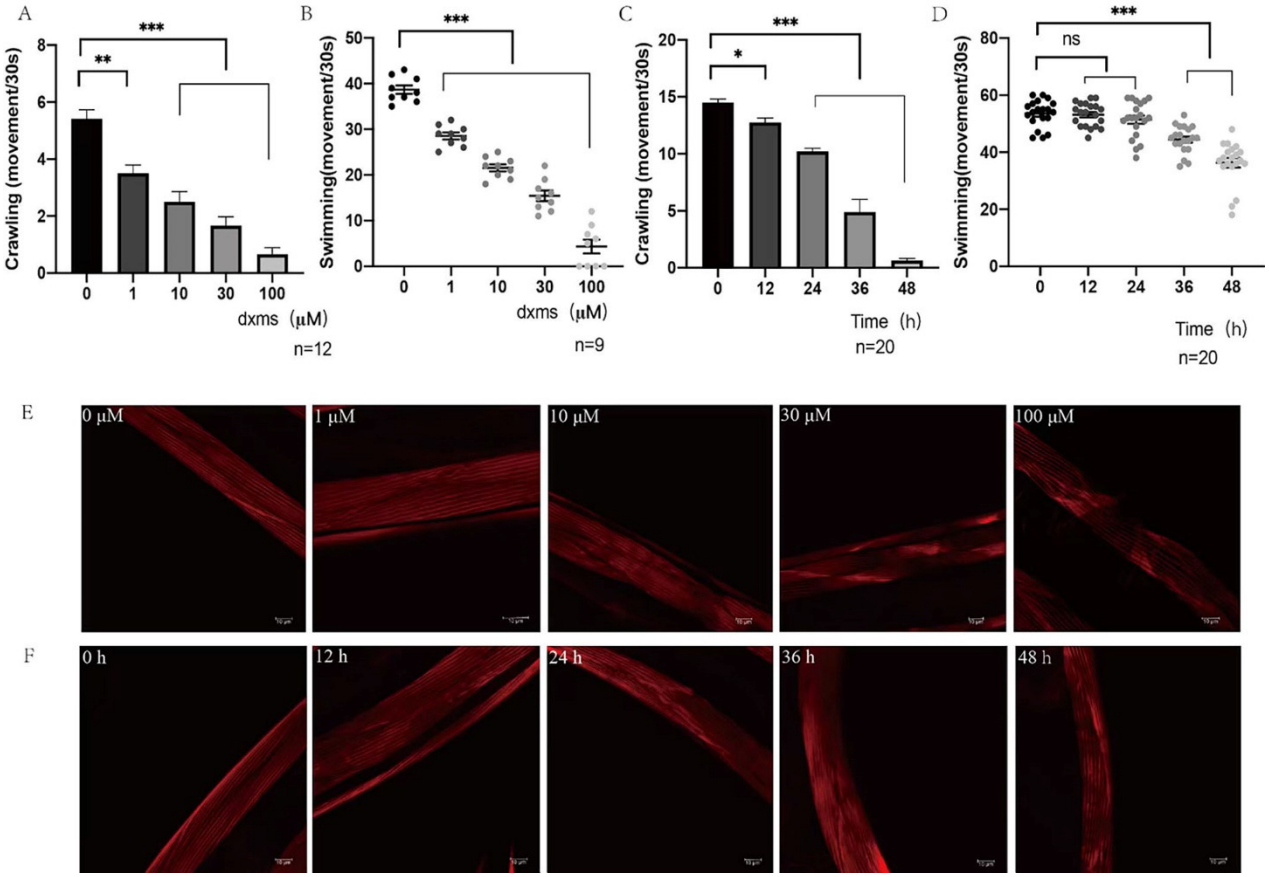

Fig. 1. Effects of dexamethasone on striated muscle structure and function in *C. elegans*. (A, B) Crawling (A) and swimming (B) frequencies of *C. elegans* treated with (0 – 100) μmol/L dexamethasone for 36 h. (C, D) Crawling (C) and swimming (D) frequencies of *C. elegans* treated with 10 μmol/L dexamethasone for (0 – 48) h. All experiments were performed at 20℃. DXMS, dexamethasone. The numbers of animals in each group are indicated in the corresponding figure. $^{*}P < 0.05$, $^{**}P < 0.01$, $^{**}{}^{*}P < 0.001$, ns means no significant difference. (E, F) *C. elegans* were treated with (0 – 100) μmol/L dexamethasone for 36 h (E) or with 10 μmol/L dexamethasone for (0 – 48) h (F). Images of rhodamine-phalloidin staining of the body wall showing F-actin myofilaments of the striated muscles.

3.2 Dexamethasone and KF-8 do not affect the reproductive ability, lifespan, and body dimensions of C. elegans

Next, we evaluated the effects of dexamethasone and KF-8 on common physiological parameters of *C. elegans* including reproduction, lifespan, and body dimensions (Fig. 2A). As shown in Figure 2B − C, neither dexamethasone nor KF-8 significantly affected the total number of eggs laid or the number of eggs laid per day by individual animals during a five-day spawning period. The survival analysis revealed no differences in lifespan between control *C. elegans* and those treated with dexamethasone and KF-8, alone or in combination (Fig. 2D − E). Body length and width are important indicators of *C. elegans* health status [31]. We detected no differences in body length or width between control *C. elegans* and those treated with dexamethasone and

KF-8, alone or in combination (Fig. 2F − G). Together, these data indicate that both dexamethasone (10 μmol/L) and KF-8 (0.05 – 0.3) mmol/L were well tolerated by *C. elegans*, showing no measurable toxicity.

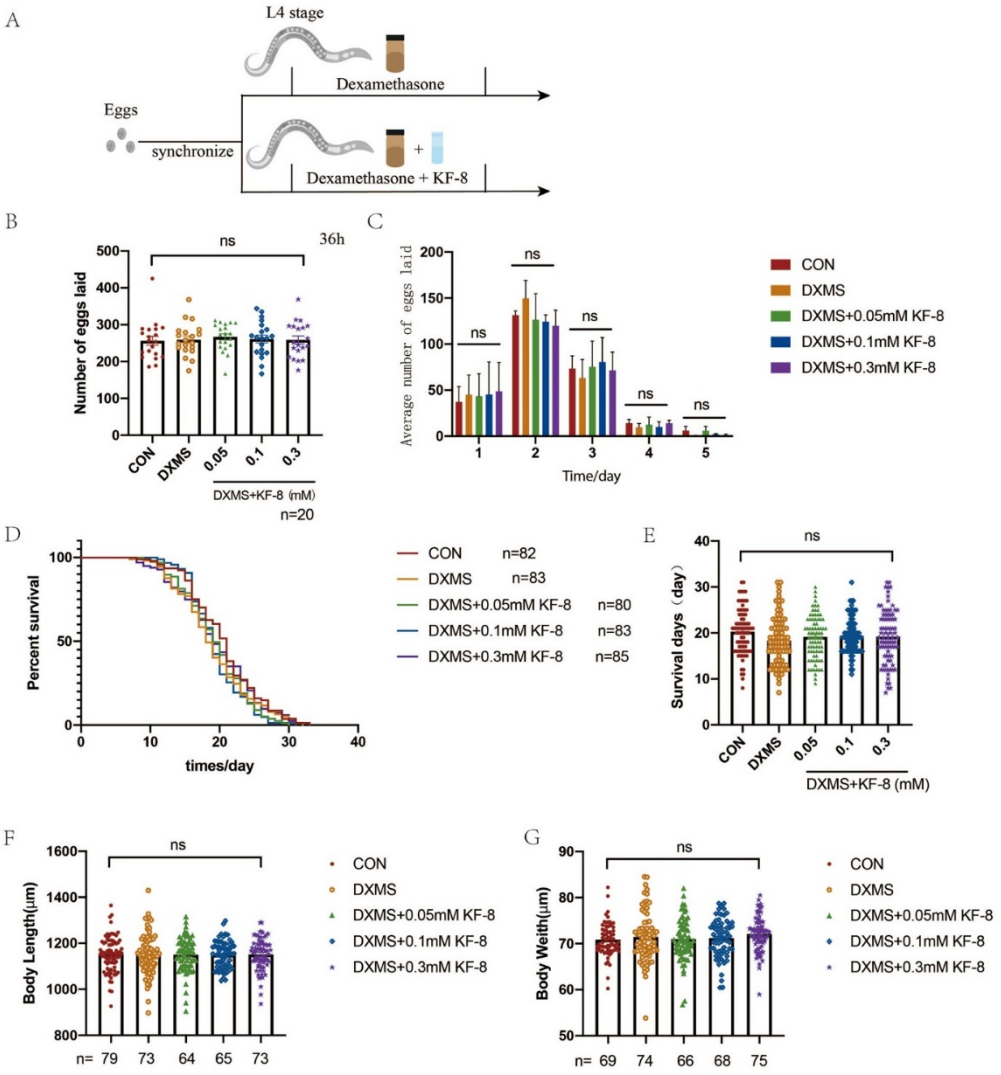

Fig. 2. Effects of dexamethasone and KF-8 on common physiological parameters of *C. elegans*. *C. elegans* were treated with dexamethasone and KF-8, alone or in combination as indicated. (A) Schematic diagram of dexamethasone and KF-8 treatment of *C. elegans*. The untreated animals were included as control. (B, C) Total number of eggs laid (B) and average number of eggs laid per day (C) by individual animals during a five-day spawning period. (D) Survival curve. (E) Lifespan of individual animals. (F) Body length of individual animals. (G) Body width of individual animals. All experiments were performed at 20°C. The numbers of animals in each group are indicated in the corresponding figure. CON, control; DXMS, dexamethasone; ns, no significant difference.

3.3 KF-8 protects against dexamethasone-induced myopathy in C. elegans

In their natural habitat, *C. elegans* need to burrow through the soil matrix for survival. Burrowing of *C. elegans* is a low-frequency, high-amplitude movement. The pharynx is a neuromuscular organ of *C. elegans* [32]. *C. elegans* feed through pharyngeal pumping, which is the regular extension and contraction of the pharynx. In addition, *C. elegans* swing their heads to search for food and explore the surrounding environment. In this study, we evaluated burrowing, pharyngeal pumping, and head swing behaviors as indicators of *C. elegans* muscle functions (Fig. 3A). Similar to its effects on crawling and swimming, 10 μmol/L dexamethasone decreased the burrowing, pharyngeal pumping, and head swing frequencies of *C. elegans*. These dexamethasone-induced losses in muscle functions were reversed by KF-8 treatment (0.05 –

0.3) mmol/L (Fig. 3B − D). Similarly, KF-8 alleviated dexamethasone-induced decreases in crawling and swimming speed and frequency (Fig. 3E − H). The muscle differentiation of nematode body walls depends on the muscle-specific transcription factors HLH-1 and UNC-54, which regulate the expression of various muscle proteins such as myosin and actin [33]. The qRT-PCR data revealed that dexamethasone downregulated HLH-1 and UNC-54, and KF-8 restored expression after dexamethasone treatment (Fig. 3I). Rhodamine-phalloidin staining showed that KF-8 prevented dexamethasone-caused myofilament disruption in striated muscles of the body wall (Fig. 3J). However, the effects of KF-8 did not increase from the medium (0.1 mmol/L) to high (0.3 mmol/L) feeding dose. This lack of dose-dependence could be attributed to the voluntary intake of the peptide as a food supplement, which could result in the loss of correlation between the amount fed and the amount actually consumed by the animal. The animals might have avoided excessive intake of KF-8 to avoid adverse effects. Accordingly, we chose to use 0.1 mmol/L KF-8 in subsequent experiments.

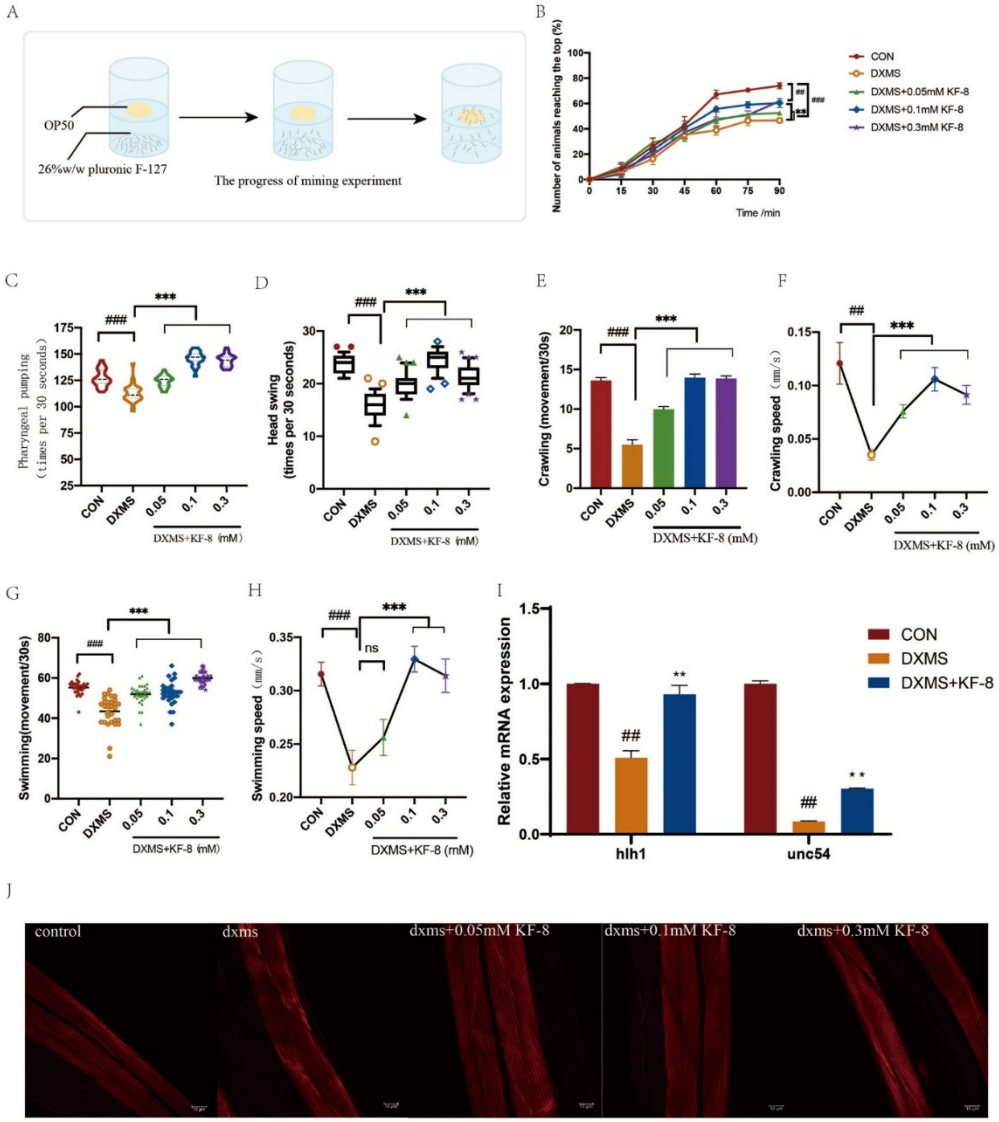

Fig. 3. Effects of dexamethasone and KF-8 on locomotor functions of *C. elegans*. *C. elegans* were treated with 10 μmol/L dexamethasone and (0.05 − 0.3) mmol/L KF-8, alone or in combination as indicated. The untreated animals were included as control. (A) Schematic diagram of burrowing experiment. (B) Burrowing ability. (C) Pharyngeal pumping frequency. (D) Head swing frequency. (E) Crawling frequency. (F) Crawling speed (G) Swimming frequency. (H) Swimming speed. (I) The mRNA expression levels of *hlh1* and *unc54* by qRT-PCR. (J) Images of rhodamine-phalloidin staining of the body wall

muscle showing F-actin myofilaments. DXMS, 10 μmol/L dexamethasone. All experiments were performed at 20℃. A, n = 30 ± 2 per group; B − G, n=30 per group; $^{**,\#\#}P < 0.01$, $^{***,\#\#\#}P < 0.001$; ns means no significant difference.

3.4 KF-8 reduces dexamethasone-induced oxidative stress in C. elegans

Oxidative stress contributes to age-related decreases in muscle mass and performance [34]. Recent studies have also demonstrated that oxidative stress is a contributing factor in dexamethasone-induced muscle atrophy in mice [35, 36]. To explore the mechanisms by which KF-8 protects against dexamethasone-induced myopathy in *C. elegans*, we assessed levels of ROS using DCFH-DA staining, a specific fluorescent probe for ROS. We also determined levels of common oxidative stress markers including MDA and T-AOC, as well as the activities of the anti-oxidant enzymes GSH-Px and SOD. As shown in Figure S1A and S1B, *C. elegans* treated with 10 μmol/L dexamethasone exhibited markedly higher fluorescence intensity of DCFH-DA staining compared to control, indicating that dexamethasone induced oxidative stress in *C. elegans*. Treatment with 0.1 mmol/L KF-8 resulted in a 28.7% drop in DCFH-DA staining intensity in the dexamethasone-treated worms (Fig. S1A − B), showing that KF-8 prevented oxidative stress caused by dexamethasone. In addition, dexamethasone increased MDA and decreased T-AOC (Fig. S1C − D). SOD and GSH-px are important antioxidant enzymes in *C. elegans* [37]. Dexamethasone inhibited the enzymatic activities of both SOD and GSH-px (Fig. S1E-F). Treatment with 0.1 mmol/L KF-8 ameliorated dexamethasone-induced changes in MDA, T-AOC, and SOD. These results were in alignment with the ROS reduction effects of KF-8 and further support KF-8 as an anti-oxidant that can reduce oxidative stress induced by dexamethasone in *C. elegans*.

3.5 Dexamethasone and KF-8 affect gene expression in C. elegans

To further explore the mechanisms of KF-8 at the molecular level, we obtained gene expression profiles of *C. elegans* treated with 10 μmol/L dexamethasone and 0.1 mmol/L KF-8, alone or in combination, using transcriptome sequencing analysis. Differentially expressed genes (DEGs) were identified based on the following criteria: 1) a fold change of more than 1.5 or less than 0.67, and 2) a *P*-value of < 0.05. A total of 104 DEGs were identified between the dexamethasone and dexamethasone + KF-8 groups. The relative expression levels of these 104 genes in the control, dexamethasone, and dexamethasone + KF-8 groups are presented in the form of a heatmap (Fig. 4A). Out of the 104 DEGs, 80 were downregulated and 24 were upregulated by KF-8 (Tables S1 and S2). The DEG data were imported to Metascope (http://metascape.org/) for pathway enrichment analysis, and the results are presented in the form of a bubble plot (Fig. 4B). The locomotion pathway involved the greatest number of DEGs. Other prominent signaling pathways included the insulin receptor signaling and the PI3K-AKT pathways. Notably, high level interactions were detected between all pathways except locomotion and cell projection assembly (Fig. 4C). The DEG data were also imported into the string database (https://string-db.org/cgi/) for protein-protein interaction functional enrichment analysis. As a result, an interactive network of 36 DEG-encoded proteins was revealed (Fig. 4D). The beneficial effects of KF-8 in *C. elegans* were likely mediated by these proteins and their interactions.

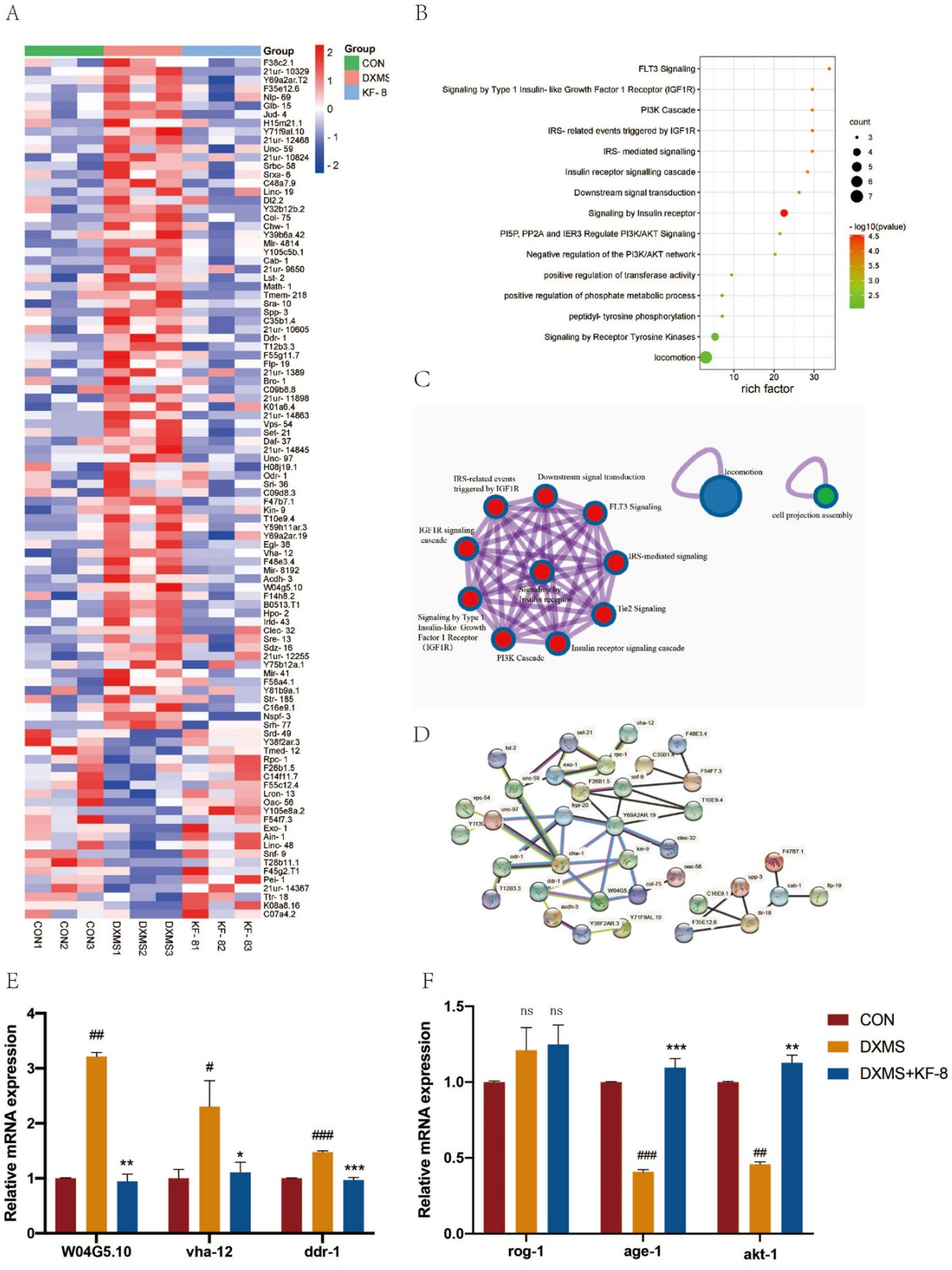

Fig. 4. DEG identification and pathway enrichment analysis. *C. elegans* were treated with 10 μmol/L dexamethasone and 0.1 mmol/L KF-8, alone or in combination as indicated. Untreated *C. elegans* were included as control. (A) Heatmap of DEGs between the dexamethasone and dexamethasone + KF-8 groups. (B) Bubble plot of DEG-based pathway enrichment analysis. The size of the dots represents the number of genes engaged. The color represents the level of association (red, high; green, low). (C) Diagram of interactions between DEG-related pathways. (D) Diagram of interactions between DEG-encoded proteins. (E) mRNA expression levels of *W04G5.10*, *vha-12*, and *ddr-1* by qRT-PCR. (F) mRNA expression levels of *rog-1*, *age-1*, and *akt-1* by qRT-PCR. CON, control; DXMS, dexamethasone. n=3; $^{\#}P < 0.05$, $^{\#\#}P < 0.01$, $^{\#\#\#}P < 0.001$ vs. control; $^{*}P < 0.05$, $^{**}P < 0.01$, $^{***}P < 0.001$ vs. DXMS; ns means no significant difference vs. control.

3.6 Dexamethasone and KF-8 regulate locomotion-related genes in C. elegans

According to transcriptome sequencing data, treatment with 10 μmol/L dexamethasone significantly increased the expression of *W04G5.10*, *vha-12*, and *ddr-1*, which have been predicted to regulate locomotion in *C. elegans* [38–40]. qRT-PCR analysis confirmed that dexamethasone upregulated expression of these genes (Fig. 4E). Treatment with 0.1 mmol/L KF-8 decreased *W04G5.10*, *vha-12*, and *ddr-1* expression in dexamethasone-treated *C. elegans* by 3.56-, 2.06-, and 1.53-fold, respectively, which were close to the 4.22-, 2.00-, and 2.50-fold decreases detected using transcriptome sequencing (Fig. S1G). Pearson correlation analysis revealed a correlation coefficient of 0.7957 between the fold changes detected from the qRT-PCR and transcriptome sequencing (Fig. S1H). Next, we evaluated the expression of *rog-1*, *age-1* (the catalytic subunit ortholog of PI3K), and *akt-1*, genes that are critical components of the insulin receptor signaling and PI3K-AKT pathways in *C. elegans*. Neither dexamethasone nor KF-8 showed significant effects on *rog-1*, however, dexamethasone downregulated both *age-1* and *akt-1*, and KF-8 treatment restored *age-1* and *akt-1* downregulated following dexamethasone treatment (Fig. 4F).

3.7 Age-1 silencing leads to locomotion dysfunction in C. elegans

To further investigate the role of *age-1* in the protective effects of KF-8, we used RNAi to knock down *age-1*. RNAi can be achieved in *C. elegans* using inactivated *E. coli* HT115 bacteria as a food source [41]. In this study, we created an HT115 strain expressing an *age-1*-targeting dsRNA (HT115 mutant). While no differences in *age-1*, *akt-1*, and *rog-1* expression were detected between animals fed the OP50 or wild type HT115 bacteria (Fig. 5A), the worms fed the mutant HT115 strain exhibited lower *age-1* and *akt-1* expression compared with those fed the wild type H115 (Fig. 5B). This was expected because *akt-1* acts downstream of *age-1* in *C. elegans* [42]. Interestingly, worms fed the mutant strain also showed lower expression of *hlh-1* and *unc54* compared with those fed the wild type strain (Fig. 5C). In the locomotor function experiments, animals fed the OP50 or wild type HT115 bacteria showed similar burrowing, crawling, and swimming abilities, but the worms fed the mutant HT115 strain exhibited decreased levels of these locomotor behaviors compared with those fed the wild type strain (Fig. 5D–5I). These results support that *age-1* and *akt-1* regulate locomotor function of *C. elegans*. Notably, KF-8 treatment of the *C. elegans* fed the mutant HT115 bacteria failed to restore the decreased expression of *age-1* or *akt-1* or recover the impaired locomotor functions in these animals. These results suggest that KF-8 prevents muscle damage caused by dexamethasone by targeting signaling pathways upstream of *age-1* and *akt-1*.

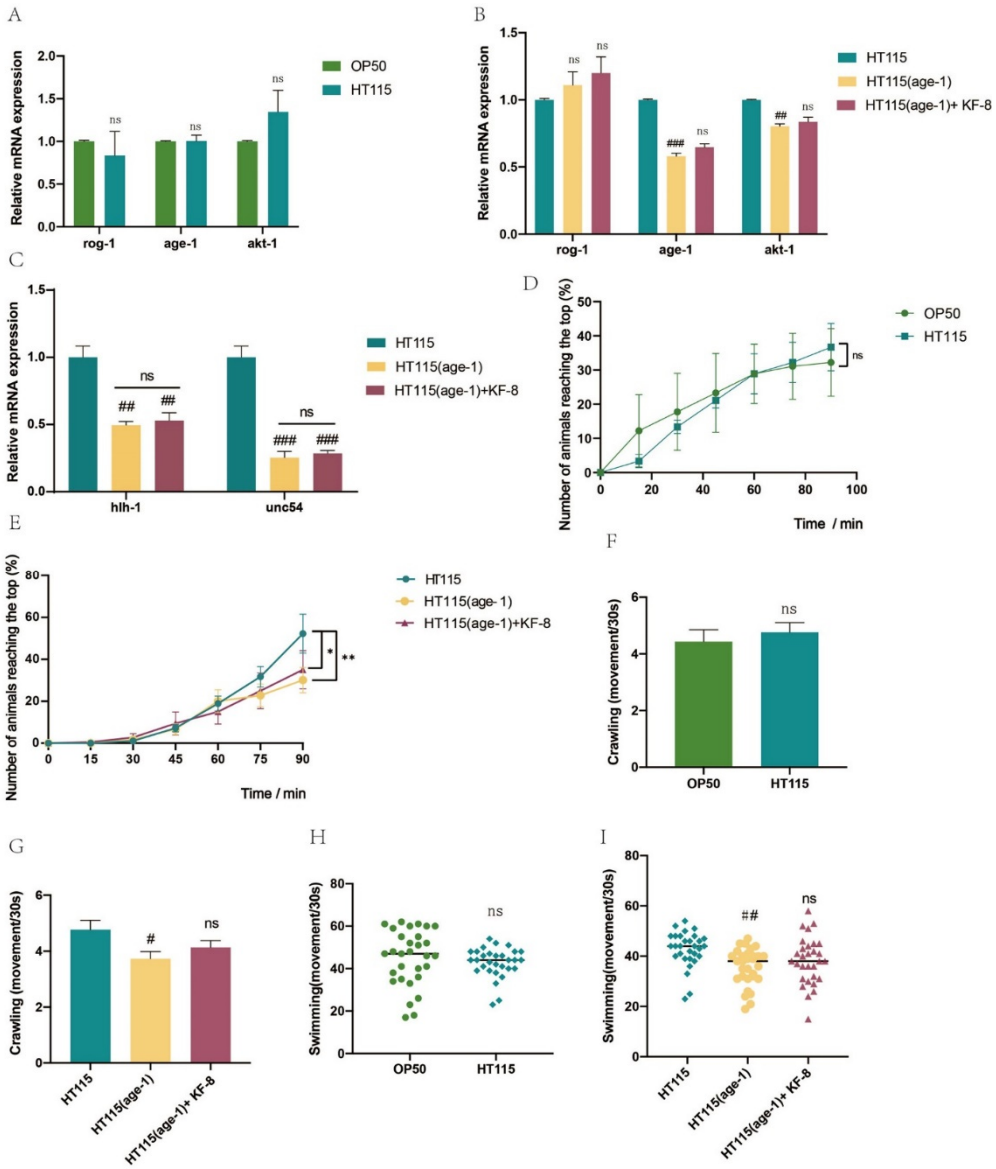

Fig. 5. *Age-1* and *akt-1* regulate locomotor functions in *C. elegans*. *C. elegans* fed the OP50, wildtype HT115, or mutant HT115 expressing *age-1*-targeting dsRNA were treated with 10 μmol/L dexamethasone and 0.1 mmol/L KF-8, alone or in combination as indicated. Untreated *C. elegans* were included as control. (A, B) mRNA expression levels of *rog-1*, *age-1*, and *akt-1* by RT-qPCR. (C) mRNA expression levels of *hlh-1* and *unc54* by RT-qPCR. (D, E) Burrowing ability. (F, G) Crawling ability. (H, I) Swimming ability. n=3; $^{*,\#}P < 0.05$, $^{**,\#\#}P < 0.01$, $^{\#\#\#}P < 0.001$ vs. HT115; ns means no significant difference vs. OP50 or HT115 mutant.

3.8 Dexamethasone and KF-8 regulate locomotion-related proteins in C2C12 myotubes via the IRS-PI3K-Akt pathways

To investigate the effects and mechanisms of action of KF-8 in mammalian muscle cells, we constructed a C2C12 myotube injury model induced by dexamethasone. C2C12 myotube formation was confirmed by myosin heavy chain 3 staining (Fig. S2A − B). We found that dexamethasone impaired C2C12 myotube formation and induced oxidative injury (Fig. S2C − D, F – K), while KF-8 enhanced myotube formation (Fig. S2E). Importantly, treatment with 30 μg/mL KF-8 restored myotube formation and reduced oxidative injury caused by 10 μmol/L dexamethasone (Fig. S2F–K). DDR-1, Flt3, and ATP6V1B2 are mammalian orthologs of *ddr-1*, *W04G5.10*, and *vha-12*, respectively. To investigate the mechanisms of action of KF-8 in C2C12 myotubes, we determined the protein expression of DDR-1, Flt3, and ATP6V1B2 using western blot analysis.

Similar to the qRT-PCR results in *C. elegans*, 10 μmol/L dexamethasone significantly upregulated DDR-1, Flt3, and ATP6V1B2 protein expression in C2C12 myotubes, and treatment with 30 μg/mL KF-8 decreased DDR-1, Flt3, and ATP6V1B2 upregulated by dexamethasone (Fig. S2L-M). The western blot analysis also showed that dexamethasone downregulated the p-IRS1/IRS, p-PI3K/PI3K, and p-Akt/Akt protein ratios, and KF-8 restored these ratios (Fig. 6A − B), supporting the IRS1-PI3K-Akt pathway as a mediator of KF-8 in C2C12 myotubes. In mammalian cells, mTOR acts downstream of Akt and upstream of 4EBP1 and p70S6K to control protein translation. Further western blot analysis revealed that dexamethasone downregulated the phosphorylation of mTOR and upregulated the phosphorylation of 4EBP1, although there were no effects on p70S6K (Fig. 6C − D). These data suggest that dexamethasone regulates DDR-1, Flt3, and ATP6V1B2 protein synthesis in C2C12 myotubes through the IRS1-PI3K-Akt-mTOR-4EBP1 pathway. Activation of the PI3K-Akt pathway is well known to downregulate FOXO1-Murf1/Atrogin-1 signaling to suppress protein degradation. In line with its downregulation of the IRS1-PI3K-Akt pathway, dexamethasone upregulated FOXO1, Murf1, and Atrogin-1 (Fig. 6E − F). These data suggest that dexamethasone also regulates DDR-1, Flt3, and ATP6V1B2 levels by activating protein degradation. Importantly, all changes in protein expression and phosphorylation caused by dexamethasone were reversed by treatment with 30 μg/mL KF-8. Finally, treatment with the PI3K inhibitor LY294002 abolished the effects of KF-8 on PI3K, Akt, mTOR, and 4EBP1 phosphorylation (Fig. 6G − H), confirming that KF-8 acts through the PI3K-Akt-mTOR-4EBP1 pathway.

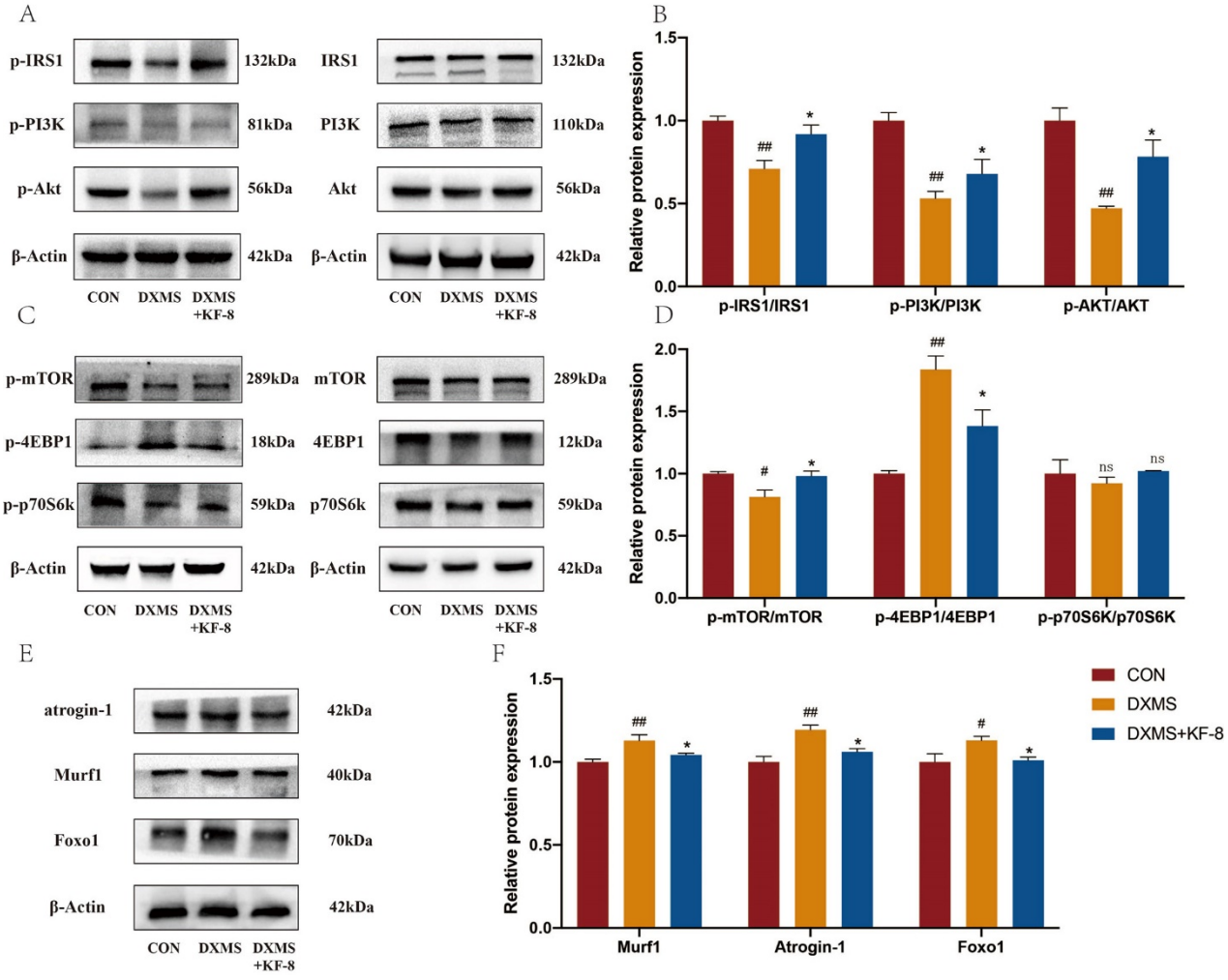

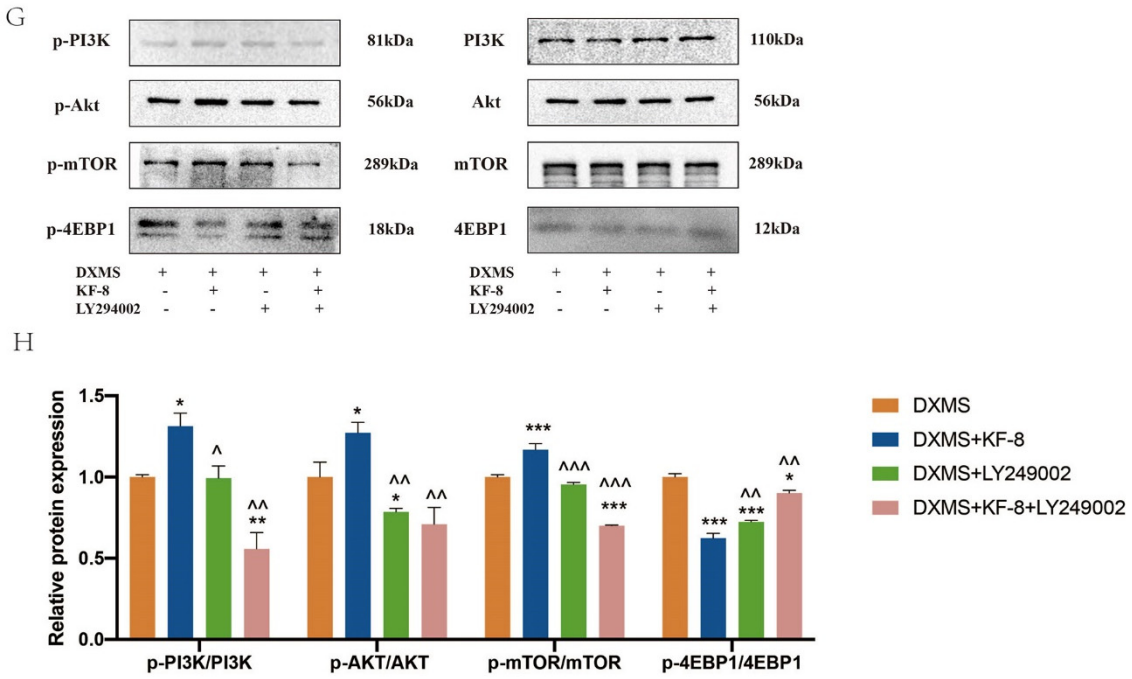

Fig. 6. Dexamethasone and KF-8 regulate locomotion-related proteins in C2C12 mouse myotubes via the IRS-PI3K-Akt pathway. C2C12 myotubes were treated with 10 μmol/L dexamethasone, 30 μg/ml KF-8, and 10 μmol/L LY294002, alone or in combination as indicated, for 48 h. Untreated cells were included as control. Intracellular protein expression was determined using western blot analysis. (A, B) Western blot images of p-IRS1, p-PI3K, and p-AKT (left panel) and IRS1, PI3K, and Akt (right panel) (A) and the corresponding phosphorylated protein to total protein ratios (B). (C, D) Western blot images of p-mTOR, p-4EBP1, and p-p70S6K (left panel) and mTOR, 4EBP1, and p70S6K (right panel) (C) and the corresponding phosphorylated protein to total protein ratios (D). (E, F) Western blot images (E) and quantified protein expression of Murf1, Atrogin-1, and Foxo1 (F). (G, H) Western blot images of p-PI3K, p-Akt, p-mTOR, and p-4EBP1 (left panel) and PI3K, Akt, mTOR, and 4EBP1 (right panel) (G) and the corresponding phosphorylated protein to total protein ratios (H). CON, control; DXMS, dexamethasone; n=3; $^{\#}P < 0.05$, $^{\#\#}P < 0.01$, $^{\#\#\#}P < 0.001$ vs. CON; $^{*}P < 0.05$, $^{**}P < 0.01$, $^{***}P < 0.001$ vs. DXMS; $^{\wedge}P < 0.05$, $^{\wedge\wedge}P < 0.01$, $^{\wedge\wedge\wedge}P < 0.001$ vs. DXMS + KF-8; ns means no significant difference vs. CON.

4. Discussion

Dexamethasone is a steroid hormone drug that is commonly used as an anti-inflammatory or an immunosuppressive agent. Muscle atrophy is a main side effect of high dose or sustained dexamethasone use. To date, no pharmaceutical interventions have been approved or recommended for the treatment of this condition. In this study, we successfully established a *C. elegans* model of dexamethasone-induced myopathy. To the best of our knowledge, this is the first report using a *C. elegans* model to investigate drug-induced myopathy. We found that dexamethasone caused actin filament disruptions in the striated muscles of the body wall, leading to defects in typical *C. elegans* locomotor behaviors such as crawling, swimming, burrowing, pharyngeal pumping, and head swing. Administration of KF-8, a bioactive peptide from rice bran, protected against dexamethasone-induced actin filament disruptions and locomotor defects. Mechanical studies with *C. elegans* and C2C12 mouse myotubes implicated locomotion-related genes and the IRS-PI3K-Akt pathway as mediators of the protective effects of KF-8.

C. elegans has a well-sequenced and annotated genome, and it has major signal transduction pathways similar to those of humans [45]. As such, *C. elegans* is a model organism for studying a number of human diseases [44]. The additional advantages of *C. elegans* as a model organism for human diseases include its short lifespan (~21 days), high offspring yield, and low maintenance cost. Moreover, research using *C. elegans* does

not require ethical approval [43]. Despite its simple living environment and limited locomotory behaviors, *C. elegans* is rarely used as a model to study myopathy. However, *C. elegans* does have certain unique advantages for muscle-related studies. Its body wall is composed of a large number of muscle cells to support its locomotion. In addition, it has a small and transparent body, which makes microscopic analysis of its muscle microstructure relatively easy. Indeed, *C. elegans* has been used to study aging-related changes in locomotor functions [46], as well as muscle structural damages and dysfunctions caused by Ca^{2+} overload [25,47]. In this study, we established the first *C. elegans* model of dexamethasone-induced myopathy. We found that dexamethasone slowed the typical locomotory movements of *C. elegans* and disrupted and bent actin filaments in the body wall muscles. These myostructural damages and functional defects induced by dexamethasone were similar to those observed in rodents and zebrafish [22, 48, 49]. Thus, the findings from this study suggest that *C. elegans* is a convenient, low-cost model to investigate dexamethasone-induced myopathy, and perhaps other types of myopathy as well. However, the use of a nematode model might limit the direct applicability of the results to human conditions, and thus the efficacy of KF-8 in protecting against dexamethasone-induced myopathy must be verified in rodent models before introducing it into a clinical trial.

Currently, protein supplements are widely used to increase muscle mass. Certain peptides have shown beneficial effects on muscle growth, as well. For example, pea peptide supplementation can increase muscle weight and thickness in rats [51]. The SP peptide extracted from silk can help recover muscle loss in mice fed a high-fat diet [52]. In addition, peptides obtained from potato hydrolysis can enhance muscle protein synthesis in C2C12 cells exposed to high glucose [53]. However, there have been very limited studies on the mechanisms of action of these peptides. In this study, we investigated the mechanisms mediating the myoprotective effects of KF-8 in *C. elegans* and C2C12 myotubes.

Elevated ROS have been implicated in a wide spectrum of human diseases. Our previous work found that KF-8 protected against oxidative stress-related organ injury in aging mice by inhibiting NF-κB/p38 signaling and preserving Nrf2 activity.[21] We also found that KF-8 extended the body length, prolonged the life span, and improved the motility of *C. elegans* by controlling oxidative stress [54]. Studies have shown that dexamethasone can induce oxidative stress in rodents, and agents with anti-oxidant properties can alleviate dexamethasone-induced myopathy by decreasing oxidative stress [55, 56]. In keeping with these findings in rodents, we found that dexamethasone increased ROS and MDA, decreased T-AOC, and decreased SOD and GSH-px activities in *C. elegans*. KF-8 inhibited the changes in the above oxidative stress-related markers induced by dexamethasone, suggesting that KF-8 may protect against dexamethasone-induced myopathy through its anti-oxidant properties. The specific pathways mediating KF-8's antioxidant activities in *C. elegans* will be addressed in our future studies. In terms of general health, neither dexamethasone nor KF-8 showed significant effects on the body length, body width, lifespan, or reproductive ability of *C. elegans*.

The transcriptome sequencing analysis identified 104 DEGs between *C. elegans* treated with dexamethasone and those treated with dexamethasone and KF-8. Enrichment analysis of the DEGs implicated the locomotion and IRS pathways as possible mediators of KF-8's myoprotection. Further qRT-PCR analysis

confirmed that dexamethasone and KF-8 regulated the locomotion-related genes *W04G5.10*, *vha-12*, and *ddr-1*. *W04G5.10* is an ortholog of mammalian Flt3. Flt3 is a receptor tyrosine kinase that was found to mediate myogenesis in C2C12 myoblasts [34]. Vha-12 is an ortholog of mammalian ATPase H+ transporting V1 subunit B2 (ATP6V1B2), a principal proton pump in mammals. ATP6V1 inadequacy has been linked to X-linked myopathy with excessive autophagy, a disease characterized by progressive atrophy of skeletal muscle [35]. In *C. elegans*, *vha-12* encodes a V-ATPase that participates in cellular endocytosis, and *vha-12* deficiency is linked to impaired clearance of apoptotic cells [57]. *Ddr-1* was detected in motor neuron axons in *C. elegans* and found to guide axon navigation and tract formation.[36] In this study, the increased expression of *W04G5.10*, *vha-12*, and *ddr-1* in response to dexamethasone may serve as a compensatory mechanism against muscle and motor neuron damage. *Hlh-1* and *unc-54* are orthologs of mammalian MYOD1 and MYH. In mammals, MYOD1 is a phosphoprotein found in the nucleus of proliferating myoblasts and differentiated myotubes, while MYH is a myosin protein. Both MYOD1 and MYH play an important role in myoblast differentiation and myotube formation [58, 59]. In this study, KF-8 restored *hlh-1* and *unc-54* downregulated by dexamethasone, highlighting the role of *hlh-1* and *unc-54* as mediators of the myoprotective effects of KF-8 in *C. elegans*. PI3K can activate MYOD to promote muscle injury repair in pigs [60]. Dexamethasone has also been shown to inhibit the phosphorylation of IRS and the downstream PI3K-Akt pathway to repress protein synthesis and accelerate protein decomposition in mammalian cells [61, 62]. In this study, dexamethasone downregulated *age-1*, the ortholog of mammalian PI3K, in *C. elegans*, and KF-8 restored *age-1* downregulated by dexamethasone, supporting *age-1* as a mediator of KF-8 in *C. elegans*, likely upstream of *hlh-1*. Importantly, the RNAi experiments using an *E. coli* HT115 strain expressing an *age-1*-targeting dsRNA confirmed that *age-1* is a critical regulator of muscle functions in *C. elegans*. We also found that dexamethasone inhibited the phosphorylation of IRS, PI3K, and Akt in C2C12 myotubes. Akt can phosphorylate mTOR to enhance protein synthesis by activating p70S6K and inhibiting 4EBP1[63]. Akt can also inhibit the transcriptional activity of Foxo to reduce protein breakdown by downregulating Atrogin-1 and MuRF1[64]. In this study, dexamethasone downregulated the Akt-mTOR-4EBP1 and Akt-Foxo-Atrogin-1/Murf1 pathways in C2C12 myotubes, and these dexamethasone-induced changes in signaling pathways were reversed by KF-8. Moreover, the PI3K inhibitor LY294002 blocked the regulation of PI3K, Akt, mTOR, and 4EBP1 phosphorylation by KF-8. These results strongly support the PI3K-Akt-mTOR-4EBP1 pathway as a mediator of KF-8 in C2C12 myotubes. However, other molecular mechanisms may also play a role in mediating the myoprotective effects of KF-8, which require further investigation.

In summary, we established the first *C. elegans* model of dexamethasone-induced myopathy. We also demonstrated that the KF-8 peptide protected against dexamethasone-induced myopathy in *C. elegans* by regulating locomotion-related genes and the IRS-PI3K-Akt pathway. These data support KF-8 as a dietary supplement to treat GC-induced myopathy in humans, but the efficacy of KF-8 needs to be verified in rodent

models before moving into clinical trials. Whether KF-8 has beneficial effects on other types of myopathy awaits future investigation.

Funding

This work was supported by funding from the National Key Research and Development Program of China (2022YFF1100203), National Natural Science Foundation of China (No.32372349), Science and Technology Innovation Talent Project of Hunan Province (No.2022RC3056), Natural Science Foundation for Distinguished Young Scholars of Hunan Province (No. 2021JJ10078).

Conflicts of Interest

None of the authors have any conflicts of interest to declare.

Data Availability

All data generated or analyzed during this study are included in this published article [and its supplementary information files].

References

[1] Wilkinson DJ, Piasecki M, Atherton PJ. The age-related loss of skeletal muscle mass and function: Measurement and physiology of muscle fibre atrophy and muscle fibre loss in humans. *Ageing Res Rev*. 2018; 47: 123–132. https://doi.org/10.1016/j.arr.2018.07.005

[2] So HK, Kim H, Lee J, You CL, Yun CE, Jeong HJ, Jin EJ, Jo Y, Ryu D, Bae GU, et al. Protein Arginine Methyltransferase 1 Ablation in Motor Neurons Causes Mitochondrial Dysfunction Leading to Age-related Motor Neuron Degeneration with Muscle Loss. *Research*. 2023; 6: 0158. https://doi.org/10.34133/research.0158

[3] Jaitovich, A., Barreiro, E. Skeletal Muscle Dysfunction in Chronic Obstructive Pulmonary Disease. What We Know and Can Do for Our Patients. *Am J Respir Crit Care Med*. 2018; 198(6): 175–186. https://doi.org/10.1164/rccm.201710-2140CI

[4] Bilgic SN, Domaniku A, Toledo B, Agca S, Weber BZC, Arabaci DH, Ozornek Z, Lause P, Thissen JP, Loumaye A, et al. EDA2R-NIK signalling promotes muscle atrophy linked to cancer cachexia. *Nature*. 2023; 617(7962): 827–834. https://doi.org/10.1038/s41586-023-06047-y

[5] Rodgers BD, Ward CW. Myostatin/Activin Receptor Ligands in Muscle and the Development Status of Attenuating Drugs. *Endocr Rev*. 2022; 43(2): 329–365. https://doi.org/10.1210/endrev/bnab030

[6] Dardevet D, Sornet C, Taillandier D, Savary I, Attaix D, Grizard J. Sensitivity and protein turnover response to glucocorticoids are different in skeletal muscle from adult and old rats. Lack of regulation of the ubiquitin-proteasome proteolytic pathway in aging. *J Clin Invest*. 1995; 96(5): 2113–2119. https://doi.org/10.1172/JCI118264

[7] Löfberg E, Gutierrez A, Wernerman J, Anderstam B, Mitch WE, Price SR, Bergström J, Alvestrand A. Effects of high doses of glucocorticoids on free amino acids, ribosomes and protein turnover in human muscle. *Eur J Clin Invest*. 2002; 32(5): 345–353. https://doi.org/10.1046/j.1365-2362.2002.00993.x

[8] Mishra S, Cosentino C, Tamta AK, Khan D, Srinivasan S, Ravi V, Abbotto E, Arathi BP, Kumar S, Jain A, et al. Sirtuin 6 inhibition protects against glucocorticoid-induced skeletal muscle atrophy by regulating IGF/PI3K/AKT signaling. *Nat Commun*. 2022; 13(1): 5415. https://doi.org/10.1038/s41467-022-32905-w

[9] Sato AY, Richardson D, Cregor M, Davis HM, Au ED, McAndrews K, Zimmers TA, Organ JM, Peacock M, Plotkin LI, et al. Glucocorticoids Induce Bone and Muscle Atrophy by Tissue-Specific Mechanisms Upstream of E3 Ubiquitin Ligases. Endocrinology. 2017; 158(3): 664–677. https://doi.org/10.1210/en.2016-1779

[10] Cea LA, Balboa E, Puebla C, Vargas AA, Cisterna BA, Escamilla R, Regueira T, Sáez JC. Dexamethasone-induced muscular atrophy is mediated by functional expression of connexin-based hemichannels. *Biochimica et Biophysica Acta (BBA) - Molecular Basis of Disease*. 2016; 1862(10): 1891–1899. https://doi.org/10.1016/j.bbadis.2016.07.003

[11] Sandri M, Sandri C, Gilbert A, Skurk C, Calabria E, Picard A, Walsh K, Schiaffino S, Lecker SH, Goldberg AL. Foxo transcription factors induce the atrophy-related ubiquitin ligase atrogin-1 and cause skeletal muscle atrophy. *Cell*. 2004; 117(3): 399–412. https://doi.org/10.1016/s0092-8674(04)00400-3

[12] Braith RW, Welsch MA, Mills RM, Keller JW, Pollock ML. Resistance exercise prevents glucocorticoid-induced myopathy in heart transplant recipients. *Med Sci Sports Exerc*. 1998; 30(4): 483–489. https://doi.org/10.1097/00005768-199804000-00003

[13] Gupta A, Gupta Y: Glucocorticoid-induced myopathy: Pathophysiology, diagnosis, and treatment. *Indian J Endocrinol Metab*. 2013; 17(5): 913–916. https://doi.org/10.4103/2230-8210.117215

[14] Surmachevska N, Tiwari V. Corticosteroid Induced Myopathy. In: *StatPearls*. StatPearls Publishing, 2022. Accessed February 6, 2023. http://www.ncbi.nlm.nih.gov/books/NBK557731/

[15] Kato H, Miura K, Nakano S, Suzuki K, Bannai M, Inoue Y. Leucine-enriched essential amino acids attenuate inflammation in rat muscle and enhance muscle repair after eccentric contraction. *Amino Acids*. 2016; 48(9): 2145–2155. https://doi.org/10.1007/s00726-016-2240-1

[16] Rodrigues G, Moraes T, Elisei L, Malta I, Dos Santos R, Novaes R, Lollo P, Galdino G. Resistance Exercise and Whey Protein Supplementation Reduce Mechanical Allodynia and Spinal Microglia Activation After Acute Muscle Trauma in Rats. Front Pharmacol. 2021; 12: 726423. https://doi.org/10.3389/fphar.2021.726423

[17] Di C, Jia W. Food-derived bioactive peptides as momentous food components: Can functional peptides passed through the PI3K/Akt/mTOR pathway and NF-κB pathway to repair and protect the skeletal muscle injury? *Crit Rev Food Sci Nutr*. 2023; 1–18. https://doi.org/10.1080/10408398.2023.2209192

[18] Li J, Ma J, Feng Q, Xie E, Meng Q, Shu W, Wu J, Bian L, Han F, Li B. Building Osteogenic Microenvironments with a Double-Network Composite Hydrogel for Bone Repair. *Research*. 2023; 6: 0021. https://doi.org/10.34133/research.0021

[19] Yu Y, Gaine GK, Zhou L, Zhang J, Wang J, Sun B. The classical and potential novel healthy functions of rice bran protein and its hydrolysates. *Crit Rev Food Sci Nutr*. 2022; 62(30): 8454–8466. https://doi.org/10.1080/10408398.2021.1929057

[20] Liang Y, Lin Q, Huang P, Wang Y, Li J, Zhang L, Cao J. Rice Bioactive Peptide Binding with TLR4 To Overcome H2O2-Induced Injury in Human Umbilical Vein Endothelial Cells through NF-κB Signaling. *J Agric Food Chem*. 2018; 66(2): 440–448. https://doi.org/10.1021/acs.jafc.7b04036

[21] Wang Y, Cui X, Lin Q, Cai J, Tang L, Liang Y. Active Peptide KF-8 from Rice Bran Attenuates Oxidative Stress in a Mouse Model of Aging Induced by d-Galactose. *J Agric Food Chem*. 2020; 68(44): 12271–12283. https://doi.org/10.1021/acs.jafc.0c04358

[22] Liu L., Koike H, Ono T, Hayashi S, Kudo F, Kaneda A, Kagechika H, Manabe I, Nakashima T, Oishi Y. Identification of a KLF5-dependent program and drug development for skeletal muscle atrophy. *Proc Natl Acad Sci U S A*. 2021; 118(35): e2102895118 (). https://doi.org/10.1073/pnas.2102895118

[23] Seto JT, Roeszler KN, Meehan LR, Wood HD, Tiong C, Bek L, Lee SF, Shah M, Quinlan KGR, Gregorevic P, et al. ACTN3 genotype influences skeletal muscle mass regulation and response to dexamethasone. *Sci Adv*. 2021; 7(27): eabg0088. https://doi.org/10.1126/sciadv.abg0088

[24] Nigon VM, Félix MA. History of research on C. elegans and other free-living nematodes as model organisms. WormBook. 2017; 2017: 1–84. https://doi.org/10.1895/wormbook.1.181.1

[25] Momma K, Homma T, Isaka R, Sudevan S, Higashitani A. Heat-Induced Calcium Leakage Causes Mitochondrial Damage in Caenorhabditis elegans Body-Wall Muscles. *Genetics*. 2017; 206(4): 1985–1994. https://doi.org/10.1534/genetics.117.202747

[26] König D, Kohl J, Jerger S, Centner C. Potential Relevance of Bioactive Peptides in Sports Nutrition. *Nutrients*. 2021; 13(11): 3997. https://doi.org/10.3390/nu13113997

[27] Oh KH, Sheoran S, Richmond JE, Kim H. Alcohol induces mitochondrial fragmentation and stress responses to maintain normal muscle function in *Caenorhabditis elegans*. *FASEB j*. 2020; 34(6): 8204–8216. https://doi.org/10.1096/fj.201903166R

[28] Lesanpezeshki L, Hewitt JE, Laranjeiro R, Antebi A, Driscoll M, Szewczyk NJ, Blawzdziewicz J, Lacerda CMR, Vanapalli SA. Pluronic gel-based burrowing assay for rapid assessment of neuromuscular health in C. elegans. *Sci Rep*. 2019; 9(1): 15246. https://doi.org/10.1038/s41598-019-51608-9

[29] Yoshioka Y, Kubota Y, Samukawa Y, Yamashita Y, Ashida H. Glabridin inhibits dexamethasone-induced muscle atrophy. *Arch Biochem Biophys*. 2019; 664: 157–166. https://doi.org/10.1016/j.abb.2019.02.006

[30] Shen S, Liao Q, Liu J, Pan R, Lee SMY, Lin L. Myricanol rescues dexamethasone-induced muscle dysfunction via a sirtuin 1-dependent mechanism. *J Cachexia Sarcopenia Muscle*. 2019; 10(2): 429–444. https://doi.org/10.1002/jcsm.12393

[31] Cho JY, Choi TW, Kim SH, Ahnn J, Lee SK. Morphological Characterization of small, dumpy, and long Phenotypes in Caenorhabditis elegans. *Mol Cells*. 2021; 44(3): 160–167. https://doi.org/10.14348/molcells.2021.2236

[32] Cook SJ, Crouse CM, Yemini E, Hall DH, Emmons SW, Hobert O. The connectome of the Caenorhabditis elegans pharynx. *J Comp Neurol*. 2020; 528(16): 2767–2784. https://doi.org/10.1002/cne.24932

[33] Bar-Lavan Y, Shemesh N, Dror S, Ofir R, Yeger-Lotem E, Ben-Zvi A. A Differentiation Transcription Factor Establishes Muscle-Specific Proteostasis in Caenorhabditis elegans. *PLoS Genet*. 2016; 12(12): e1006531. https://doi.org/10.1371/journal.pgen.1006531

[34] Qaisar R, Bhaskaran S, Ranjit R, Sataranatarajan K, Premkumar P, Huseman K, Van Remmen H. Restoration of SERCA ATPase prevents oxidative stress-related muscle atrophy and weakness. *Redox Biol*. 2019; 20: 68–74. https://doi.org/10.1016/j.redox.2018.09.018

[35] Yoshikawa M, Hosokawa M, Miyashita K, Nishino H, Hashimoto T. Effects of Fucoxanthin on the Inhibition of Dexamethasone-Induced Skeletal Muscle Loss in Mice. *Nutrients*. 2021; 13(4): 1079. https://doi.org/10.3390/nu13041079

[36] Kim YI, Lee H, Nirmala FS, Seo HD, Ha TY, Jung CH, Ahn J. Antioxidant Activity of Valeriana fauriei Protects against Dexamethasone-Induced Muscle Atrophy. *Oxid Med Cell Longev*. 2022; 2022: 3645431. https://doi.org/10.1155/2022/3645431

[37] Shi Y, Meng X, Zhang J. Multi- and trans-generational effects of N-butylpyridium chloride on reproduction, lifespan, and pro/antioxidant status in Caenorhabditis elegans. *Sci Total Environ*. 2021; 778: 146371. https://doi.org/10.1016/j.scitotenv.2021.146371

[38] Ge Y, Waldemer RJ, Nalluri R, Nuzzi PD, Chen J. Flt3L is a novel regulator of skeletal myogenesis. *J Cell Sci*. 2013; 126(Pt15): 3370–3379. https://doi.org/10.1242/jcs.123950

[39] Ramachandran N, Munteanu I, Wang P, Ruggieri A, Rilstone JJ, Israelian N, Naranian T, Paroutis P, Guo R, Ren ZP, et al. VMA21 deficiency prevents vacuolar ATPase assembly and causes autophagic vacuolar myopathy. *Acta Neuropathol*. 2013; 125(3): 439–457. https://doi.org/10.1007/s00401-012-1073-6

[40] Unsoeld T, Park JO, Hutter H. Discoidin domain receptors guide axons along longitudinal tracts in C. elegans. *Dev Biol*. 2013; 374(1): 142–152. https://doi.org/10.1016/j.ydbio.2012.11.001

[41] Baumanns S, Beis DM, Wenzel U. RNA-interference in the nematode Caenorhabditis elegans is effective using paraformaldehyde-inactivated E. coli HT115 bacteria as a food source. *Biochim Biophys Acta Mol Cell Res*. 2023; 1870(1): 119375. https://doi.org/10.1016/j.bbamcr.2022.119375

[42] Paradis S, Ruvkun G. Caenorhabditis elegans Akt/PKB transduces insulin receptor-like signals from AGE-1 PI3 kinase to the DAF-16 transcription factor. *Genes Dev*. 1998; 12(16): 2488–2498. https://doi.org/10.1101/gad.12.16.2488

[43] Shen P, Yue Y, Zheng J, Park Y. Caenorhabditis elegans: A Convenient In Vivo Model for Assessing the Impact of Food Bioactive Compounds on Obesity, Aging, and Alzheimer's Disease. Annu Rev Food Sci Technol. 2018 Mar 25;9:1-22. doi: 10.1146/annurev-food-030117-012709.

[44] Culetto E, Sattelle DB. A role for Caenorhabditis elegans in understanding the function and interactions of human disease genes. *Hum Mol Genet*. 2000; 9(6): 869–877. https://doi.org/10.1093/hmg/9.6.869

[45] C. elegans Sequencing Consortium: Genome sequence of the nematode C. elegans: a platform for investigating biology. *Science*. 1998; 282(5396): 2012–2018. https://doi.org/10.1126/science.282.5396.2012

[46] Ryu D, Mouchiroud L, Andreux PA, Katsyuba E, Moullan N, Nicolet-Dit-Félix AA, Williams EG, Jha P, Lo Sasso G, Huzard D, et al. Urolithin A induces mitophagy and prolongs lifespan in C. elegans and increases muscle function in rodents. *Nat Med*. 2016; 22(8): 879–888. https://doi.org/10.1038/nm.4132

[47] Sudevan S, Takiura M, Kubota Y, Higashitani N, Cooke M, Ellwood RA, Etheridge T, Szewczyk NJ, Higashitani A. Mitochondrial dysfunction causes Ca $^{2+}$ overload and ECM degradation–mediated muscle damage in *C. elegans*. *FASEB j*. 2019; 33(8): 9540–9550. https://doi.org/10.1096/fj.201802298R

[48] Fappi A, Neves J de C, Sanches LN, Massaroto E Silva PV, Sikusawa GY, Brandão TPC, Chadi G, Zanoteli E. Skeletal Muscle Response to Deflazacort, Dexamethasone and Methylprednisolone. *Cells*. 2019; 8(5): 406. https://doi.org/10.3390/cells8050406

[49] Ryu B, Je JG, Jeon YJ, Yang HW. Zebrafish Model for Studying Dexamethasone-Induced Muscle Atrophy and Preventive Effect of Maca (Lepidium meyenii). *Cells*. 2021; 10(11): 2879. https://doi.org/10.3390/cells10112879

[50] Wang Y, Guo K, Wang Q, Zhong G, Zhang W, Jiang Y, Mao X, Li X, Huang Z. Caenorhabditis elegans as an emerging model in food and nutrition research: importance of standardizing base diet. Crit Rev Food Sci Nutr. 2022 Oct 6:1-19. doi: 10.1080/10408398.2022.2130875

[51] Jia S, Wu Q, Wang S, Kan J, Zhang Z, Zhang X, Zhang X, Li J, Xu W, Du J, Wei W. Pea Peptide Supplementation in Conjunction With Resistance Exercise Promotes Gains in Muscle Mass and Strength. Front Nutr. 2022 Jul 7;9:878229. doi: 10.3389/fnut.2022.878229

[52] Lee K, Jin H, Chei S, Oh HJ, Lee JY, Lee BY. Effect of Dietary Silk Peptide on Obesity, Hyperglycemia, and Skeletal Muscle Regeneration in High-Fat Diet-Fed Mice. Cells. 2020 Feb 6;9(2):377. doi: 10.3390/cells9020377

[53] Chen YJ, Chang CF, Angayarkanni J, Lin WT. Alcalase Potato Protein Hydrolysate-PPH902 Enhances Myogenic Differentiation and Enhances Skeletal Muscle Protein Synthesis under High Glucose Condition in C2C12 Cells. Molecules. 2021 Oct 30;26(21):6577. doi: 10.3390/molecules26216577

[54] Cai J, Chen Z, Wu Y, Chen Y, Wang J, Lin Q, Liang Y. The rice bran peptide KF-8 extends the lifespan and improves the healthspan of Caenorhabditis elegans via skn-1 and daf-16. *Food Funct*. 2022; 13(5): 2427–2440. https://doi.org/10.1039/d1fo03718h

[55] Oh S, Choi CH, Lee BJ, Park JH, Son KH, Byun K. Fermented Oyster Extract Attenuated Dexamethasone-Induced Muscle Atrophy by Decreasing Oxidative Stress. *Molecules*. 2021; 26(23): 7128. https://doi.org/10.3390/molecules26237128

[56] Seo E, Truong CS, Jun HS. Psoralea corylifolia L. seed extract attenuates dexamethasone-induced muscle atrophy in mice by inhibition of oxidative stress and inflammation. *J Ethnopharmacol*. 2022; 296:115490. https://doi.org/10.1016/j.jep.2022.115490

[57] Ernstrom GG, Weimer R, Pawar DRL, Watanabe S, Hobson RJ, Greenstein D, Jorgensen E.M. V-ATPase V1 Sector Is Required for Corpse Clearance and Neurotransmission in *Caenorhabditis elegans*. *Genetics*. 2012; 191(2): 461–475. https://doi.org/10.1534/genetics.112.139667

[58] Tapscott SJ, Davis RL, Thayer MJ, Cheng PF, Weintraub H, Lassar AB. MyoD1: a nuclear phosphoprotein requiring a Myc homology region to convert fibroblasts to myoblasts. *Science*. 1988; 242(4877): 405–411. https://doi.org/10.1126/science.3175662

[59] Choi S, Jeong HJ, Kim H, Choi D, Cho SC, Seong JK, Koo SH, Kang JS. Skeletal muscle-specific Prmt1 deletion causes muscle atrophy via deregulation of the PRMT6-FOXO3 axis. *Autophagy*. 2019; 15(6): 1069–1081. https://doi.org/10.1080/15548627.2019.1569931

[60] Jing Y, Gan M, Xie Z, Ma J, Chen L, Zhang S, Zhao Y, Niu L, Wang Y, Zhu L, Shen L. Characteristics of microRNAs in Skeletal Muscle of Intrauterine Growth-Restricted Pigs. *Genes (Basel)*. 2023; 14(7): 1372. https://doi.org/10.3390/genes14071372

[61] Meng Q, Qi X, Chao Y, Chen Q, Cheng P, Yu X, Kuai M, Wu J, Li W, Zhang Q, et al. IRS1/PI3K/AKT pathway signal involved in the regulation of glycolipid metabolic abnormalities by Mulberry (Morus alba L.) leaf extracts in 3T3-L1 adipocytes. *Chin Med*. 2020; 15: 1. https://doi.org/10.1186/s13020-019-0281-6

[62] Kuo T, Lew MJ, Mayba O, Harris CA, Speed TP, Wang JC. Genome-wide analysis of glucocorticoid receptor-binding sites in myotubes identifies gene networks modulating insulin signaling. *Proc Natl Acad Sci U S A*. 2012; 109(28): 11160–11165. https://doi.org/10.1073/pnas.1111334109

[63] Zheng R, Huang S, Zhu J, Lin W, Xu H, Zheng X. Leucine attenuates muscle atrophy and autophagosome formation by activating PI3K/AKT/mTOR signaling pathway in rotator cuff tears. *Cell Tissue Res*. 2019; 378(1): 113–125. https://doi.org/10.1007/s00441-019-03021-x

[64] O'Neill BT, Lee KY, Klaus K, Softic S, Krumpoch MT, Fentz J, Stanford KI, Robinson MM, Cai W, Kleinridders A, et al. Insulin and IGF-1 receptors regulate FoxO-mediated signaling in muscle proteostasis. *J Clin Invest*. 2016; 126(9): 3433–3446. https://doi.org/10.1172/JCI86522